ISSN 1330-3651 (Print), ISSN 1848-6339 (Online)
https://doi.org/10.17559/TV-20230926000964
Original scientific paper

Seismic Signal Denoising Based on Surelet Transform for Energy Exploration

Mu DING

Abstract: Seismic signals are critical for subsurface energy exploration like oil, coal, and natural gas. Processing these signals while minimizing environmental impacts is crucial but lacking in several appropriate multi-scale geometric analysis (MGA) techniques. This study proposes using the Surelet transform, based on Stein's unbiased risk estimate (SURE), for seismic denoising. The method combines SURE to find optimal thresholds and linear expansion for coefficient estimation. Experiments on two-dimensional (2D) and three-dimensional (3D) synthetic seismic data showed Surelet achieved higher peak signal-to-noise ratios (PSNR) and faster processing compared to wavelet, curvelet, and wave atom. For example, with 20% noise, Surelet improved PSNR by 6.11% and reduced time by 78.4% versus wave atom. The feasibility of the proposed technique for efficient seismic denoising was demonstrated, highlighting implications for enabling cleaner signals in energy exploration.

Keywords: energy exploration; multi-scale geometric analysis; surelet transform; seismic signal denoising; peak signal to noise ratio

1 INTRODUCTION

Energy exploration, including oil exploration, coalfield exploration and natural gas exploration, is a means of obtaining important economic lifelines of the country. Among them, seismic exploration is an essential component of petroleum exploration, and high-quality seismic signals can discover underground geological information and obtain a large amount of effective energy [1]. However, seismic signals collected often contain noise in field seismic exploration. Noise reduction of the noisy seismic signal can more clearly and truly reflect the geological structure information. According to the characteristics of noise on the seismic section, noise is divided into coherent noise and random noise [2]. Coherent noise is regularly superimposed on the effective signal in time, showing obvious kinematics. Sound waves, surface waves and multiple waves are all coherent noise. Random noise is formed by a mixture of various unknown elements, which is relatively random in terms of its appearance [3]. The removal of random noise is generally difficult because its apparent velocity is uncertain and the frequency band is still relatively wide. In general, random noise removal is a significant subject in signal processing [4].

We have learned that petroleum exploration mainly includes seismic exploration and geochemistry exploration [5], etc. This study focuses on seismic exploration. Seismic exploration is mainly divided into three parts: seismic signal acquisition; seismic signal processing [6]; and seismic signal interpretation [7]. The denoising of seismic signals is the key step in seismic signal processing. There are two common methods for denoising seismic signals: the spatial domain and the transform domain. Among the commonly used approaches in the spatial domain are mean filtering, median filtering, and Wiener filtering [8]. These methods have certain denoising performance, but each has its own drawbacks. Common methods in transform domain include Fourier transform, wavelet transform [9, 10], K-L transform and radon transform denoising, etc. With the advancement of sparse signal constraints and compressed sensing theory in recent years, the above theory has been applied to seismic signal denoising [11]. In the current seismic signal denoising domain, multi-scale geometric analysis denoising has received extensive attention. Classical algorithms include Bandelet transform [12], Curvelet transform [13], Contourlet transform [14], and Shearlet transform [15]. This study used Surelet transform to denoise seismic signals and achieved ideal results. Surelet transform can make the denoised seismic signal as close as possible to the original seismic signal. Due to the ability of clear seismic signals to reflect actual geological structure in the field, seismic signal denoising based on Surelet transform plays a vital role in energy exploration.

The objective of this study is to find an excellent multi-scale geometric analysis method for seismic signal denoising tasks in energy exploration. (1) to apply Surelet transform to energy exploration; and (2) to take into account the performance advantage of the Surelet transform in the high peak signal-to-noise ratio and fast denoising speed.

This study makes several contributions to filling the energy exploration knowledge gap in the literature. (1) this study applies Surelet transform to energy exploration to reduce the environmental impact; (2) this study reflects the performance advantage of the suggested approach in the high peak signal-to-noise ratio and speed up the denoising process; (3) this study contributes to the seismic exploration part of energy exploration.

The structure of this paper is arranged as follows. Section 2 is the literature review, and the methods and principles of Surelet transform denoising are provided in Section 3. The results and discussion are displayed in Section 4 and Section 5 is the conclusion.

2 LITERATURE REVIEW

2.1 Energy Exploration

The development of petroleum industry faces the dual challenges of "underground" and "on the ground". From the perspective of "underground", problems such as inferior resources and complicated exploration objects have intensified. Strengthen the technology and talent reserves in the frontier areas such as conventional oil and gas, deep-water oil and gas and combustible ice, and actively build a green energy supply system. Tseng et al. [16, 17] argued that green supply chain should be emphasized. Non-polluting energy exploration coincides with the idea of green energy supply system. Energy exploration includes traditional oil seismic exploration, coalfield exploration, natural gas exploration, etc., as well as new energy exploration such as wind, solar, and bioenergy [18]. Seismic exploration is one of the most common and crucial approaches in petroleum exploration. In seismic signal processing, there are many processing

steps, such as seismic signal velocity analysis, noise removal, energy balance, stacking, deconvolution, migration. Seismic signal denoising is a critical step due to increase the signal-to-noise ratio of seismic signals. If the performance of seismic signal denoising is good, it is very helpful to explore the petroleum geological structure. Therefore, it is very crucial to find an algorithm that can precisely improve the peak signal-to-noise ratio of seismic signals. After that, energy exploration can proceed smoothly.

2.2 Multi-Scale Geometric Analysis

Wavelet transform is commonly employed in various fields, and has become another effective tool after Fourier transform. However, it cannot effectively represent the geometric features such as edges and textures with multi-directionality since the wavelet transform can only reflect the point singularity of the signal. In fact, the signals with line or surface singularity are very ordinary in high-dimensional space. Therefore, wavelet is not the optimal signal representation method [19]. Multi-scale geometric analysis has been proposed and quickly become a hot topic in current research, which is committed to developing a new optimal representation for high-dimensional signals. Multi-scale geometric analysis is divided into adaptive and non-adaptive. The former means that the basis function of the signal transformation varies with the content of the signal, including Brushlet, Wedgelet and Bandelet transform. The latter means that the basis function of the signal transformation is independent of the signal content, mainly including Ridgelet, Curvelet and Contourlet transform.

For instance, the Brushlet transform [20] is an adaptive frequency band segmentation method that is well suited for describing periodic signals, but does not provide a sparse representation for the edges of a sliced smooth signal. Donoho [21] proposed the Wedgelet transform. It is a simple and effective signal representation, which defines a piecewise binary function on a square area. A series of Wedgelets of different sizes and orientations can approximate the edge contour of the signal. Le and Mallat [22] proposed the sparsity of the Bandelet transform. It is an edge-based signal representation that can adaptively track the geometric regular direction of the signal. The central idea of constructing a Bandelet transform is to define the geometric features as vector fields rather than as a collection of ordinary edges. The Bandelet base is not predetermined, but adaptively selects the composition of the specific base by optimizing the final application results.

Candès [23] gave the basic theoretical framework of Ridgelet transform, which is a non-adaptive representation of high-dimensional signals. Donoho [24] gave a construction method of orthogonal ridge waves. Candès [25] proposed a single-scale Ridgelet transform and gave its construction method. The purpose of proposing a single-scale ridge wave is to solve the sparse approximation problem of multidimensional signal with singular curves. The Curvelet transform was suggested by Candès and Donoho [25], which was derived from the theory of ridge wave. Actually, the Curvelet transform is a special filtering process combined with multiscale Ridgelet transform [27]. Do and Vetterli [28] proposed a new representation for two-dimensional signals, Contourlet transform, also known as the Pyramidal directional filter bank (PDFB). It is a kind of multi-resolution, localized, directional signal representation. It inherits the anisotropic scale relationship of the Curvelet transform. Firstly, the signal is multi-scaled by the Laplacian pyramid transform to "capture" the point singularity, followed by the directional filter bank. The singular points distributed in the same direction are combined into one coefficient. The result of the Contourlet transform is to approximate original signal with a base structure similar to the Contour segment, which is why it is called the Contourlet transform.

2.3 Denoising Method Based on Multi-Scale Geometric Analysis

Multi-scale geometric analysis has been widely used in the field of image denoising. In Bandelet domain, for example, Zhang et al. [29] combined edge detection and feature clustering. Sadreazami et al. [30] introduced a novel image denoising algorithm in the contourlet domain. Zhang [31] suggested an algorithm for reducing noise in images that employs generalized cross validation and partial differential equations model in the tetrolet domain. Yang et al. [32] proposed an adaptive contourlet transform for denoising which combines hidden Markov model and pulse-coupled neural network. Wang et al. [33] described a denoising and augmentation approach based on non-subsampled contourlet transform and BM3D. The fused photon counting image was then subjected to an enhanced BM3D using the inverse transform, considerably lowering the operation time. The proposed method produced better results than comparison approaches in terms of various assessment metrics, as well as positive visual effects from the subjective feeling.

Due to the advantages of various multi-scale geometric analysis methods in image denoising, scholars have widely applied them in seismic signal denoising. To avoid undesirable non-smooth artifacts brought on by the curvelet transform, Tang and Ma [34] combined the projected TV approach with curvelet transform to denoise the seismic data. Al-Marzouqi and AlRegib [35] presented a learning-based approach by improving the curvelet transform. The experiments show that this approach has significant numerical and visual performance advantages compared to traditional curvelet transform. Bai et al. [36] proposed a new noise attenuation method based on least-squares Gaussian beam transform (LSGBT). The final experiments show that the performance of seismic data denoising is good. In the current research of seismic data denoising, combining some algorithms may improve the denoising performance.

For instance, Zhang et al. [37] discussed the convex set projection algorithm (POCS) applied on the basis of curvelet transform, and then a method for simultaneous reconstruction and denoising of 3D seismic data is realized. It is effective in comparison with Fourier transform method. Zhang and Vanderbaan [38] used a simplified polarization analysis in the 3D shearlet transform to build an effective micro seismic data denoising approach. Tang et al. [39] proposed the adaptive threshold shearlet transform for surface micro seismic data denoising. The experimental denoising results of seismic records show that the suggested method outperforms the conventional shearlet denoising method in retaining valid signal.

Surelet transform is an excellent algorithm for solving indefinite equations with faster calculation efficiency. It has been used in many fields such as image processing, signal reconstruction and computer vision. SURE-LET

was first proposed for image denoising [40], and demonstrated good denoising performance. SURE, approximation based on orthogonal wavelet thresholds between scales is also used for image denoising [41]. In literature, a non-adaptive image denoising approach based on Stein unbiased risk estimation linear expansion threshold is proposed, which is implemented in the non-subsampled Contourlet transform domain [42]. The SURE and LET make the denoising algorithm only solve a linear equation system, which is fast and effective.

Considering that the Surelet transform has better performance, it has the potential to solve many engineering problems. This study applies it to seismic signal denoising. Based on the unbiased risk estimation, the proposed algorithm uses the linear expansion of the threshold to solve the equations. Firstly, the signal is converted into transform domain coefficients. Then the noise contained in coefficients is removed. Finally, the inverse transform is used to obtain denoised seismic signal. Experiments show that this algorithm works well.

3 METHODS

3.1 Surelet Transform for Seismic Signal Denoising

The unbiased risk estimate is an unbiased estimate of the mean squared error (MSE) between the original signal and the denoised signal. The minimum value of the estimate is sought to minimize the MSE of original and denoised signals, which is consistent with the general purpose of denoising. Given a noise model $y_n = x_n + b_n (n = 1,...,N)$, x_n is a clear signal, b_n is a Gaussian white noise with a variance of σ^2 , and an estimate $\hat{x}$ about $x = \{x_n\}_{n=1,2,...,N}$ needs to be found, such that Eq. (1) is minimized:

$$M_{SE} = \frac{1}{N}\sum_{n=1}^{N} |\hat{x}_n - x_n|^2 \tag{1}$$

where $\hat{x} = f(y) = (\rho_n(y))_{n=1,2,...,N}$. Let the N-dimensional vector signal $f(y)$ satisfy $E\{|\partial \rho_n(y)/\partial y_n|\} < \infty$, $n = 1,2,...,N$ (differentiability), and under assumption of additive white Gaussian noise, $f(y)^T x$ with $f(y)^T - \sigma^2 \mathrm{div}\{f(y)\}$ have same expectation.

$$E\left\{\sum_{n=1}^{N} \rho_n(y) x_n\right\} = E\left\{\sum_{n=1}^{N} \rho_n(y) y_n\right\} - \sigma^2 E\left\{\sum_{n=1}^{N} \frac{\partial \rho_n(y)}{\partial y_n}\right\} \tag{2}$$

Substituting Eq. (2) into Eq. (1) yields a SURE unbiased risk estimate. The unbiased estimate of MSE is a random variable.

$$\varepsilon = \frac{1}{N}\|f(y) - y\|^2 + \frac{2\sigma^2}{N}\mathrm{div}\{f(y)\} - \sigma^2 \tag{3}$$

$$E\{\varepsilon\} = \frac{1}{N} E\{\|f(y) - x\|^2\} \tag{4}$$

Definition $f(y)$ is a linear combination of primitive denoising process $f_k(y)$,

$$f(y) = \sum_{k=1}^{K} a_k f_k(y) \tag{5}$$

The unknown weight a_k is specified by minimizing the SURE given by Eq. (3). The limitation of the LET method is that the elementary denoising process $f(y)$ satisfies the differentiability condition. In order to make the variance of SURE as small as possible, there should not be too many parameters. Since SURE is quadratic in $f(y)$, the linearity of expansion Eq. (5) is critical to solving the minimization problem. a_k is the solution of linear system $\boldsymbol{Ma} = \boldsymbol{c}$.

$$\sum_{l=1}^{K} f_k(y)^T f_l(y) a_l = f_k(y)^T y - \sigma^2 \mathrm{div}\{f_k(y)\}, \quad k = 1,2,...,K \tag{6}$$

Among them, $f_k(y)^T f_l(y) = \boldsymbol{M}_{k,l}$ and $f_k(y)^T y - \sigma^2 \mathrm{div}\{f_k(y)\} = \boldsymbol{c}_k$. Since the minimum value of ε is always present, it is guaranteed that the linear system has a solution.

$$\boldsymbol{Ma} = \boldsymbol{c} \tag{7}$$

$$\boldsymbol{a} = \boldsymbol{M}^{-1}\boldsymbol{c} \tag{8}$$

Eq. (7) and Eq. (8) are the weights when the MSE obtains the minimum value. When $\mathrm{rank}(\boldsymbol{M}) < K$, f is over-parameterized. Therefore, several sets of parameters will produce the same result. In this case, the pseudo inverse of $\boldsymbol{M}$ is considered, and the K value can also be reduced to make matrix $\boldsymbol{M}$ full rank.

3.2 Seismic Signal Denoising Based on Surelet Transform

The Surelet transform is simple, and it is easier to achieve the best theoretical performance. Therefore, it is used in seismic signal denoising. Transform domain denoising includes a pair of linear transform D-decomposition and R-reconstruction. The flow chart of seismic signal denoising appears in Fig. 1.

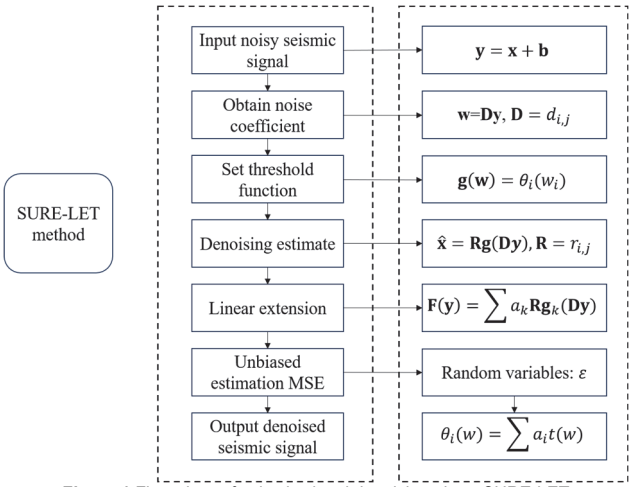

Figure 1 Flow chart of seismic signal denoising about SURE-LET

Fig. 1 presents the main steps of Stein's unbiased risk estimation linear extended threshold algorithm (SURE-LET) for seismic signal denoising are as follows:

(1) Given a noisy seismic signal $\boldsymbol{y} = \boldsymbol{x} + \boldsymbol{b}$;

(2) Matrix $\boldsymbol{D} = (d_{i,j})_{(i,j)\in[1;L]\times[1;N]}$ is applied to noisy signal to obtain a transformed noise coefficient $\boldsymbol{w} = \boldsymbol{D}\boldsymbol{y} = (w_i)_{i\in[1;L]}$;

(3) Set point-by-point threshold function $\boldsymbol{g}(\boldsymbol{w}) = (\theta_i(w_i))_{i\in[1;L]}$;

(4) Reverting to original domain by applying $\boldsymbol{R} = (r_{i,j})_{(i,j)\in[1;N]\times[1;L]}$ to the threshold function $\boldsymbol{g}(\boldsymbol{w})$, results in a denoising estimate $\hat{\boldsymbol{x}} = \boldsymbol{R}\boldsymbol{g}(\boldsymbol{w})$, which is generalized as a function of noise input coefficients

$$\hat{\boldsymbol{x}} = \boldsymbol{F}(\boldsymbol{y}) = \boldsymbol{R}\boldsymbol{g}(\boldsymbol{D}\boldsymbol{y}) \tag{9}$$

(5) Denote $\boldsymbol{F}$ as a linear extension of $\boldsymbol{F}_k$, $\boldsymbol{F}(\boldsymbol{y}) = \sum_{k=1}^{K} a_k \boldsymbol{R}\boldsymbol{g}_k(\boldsymbol{D}\boldsymbol{y})$,where $\boldsymbol{F}_k(\boldsymbol{y}) = \boldsymbol{R}\boldsymbol{g}_k(\boldsymbol{D}\boldsymbol{y})$

(6) Unbiased estimation of MSE between original and denoised signals by random variables as follows:

$$\varepsilon = \frac{1}{N}\left\|\boldsymbol{F}(\boldsymbol{y}) - \boldsymbol{y}\right\|^2 + \frac{2\sigma^2}{N}\boldsymbol{\alpha}^T \boldsymbol{g}'(\boldsymbol{D}\boldsymbol{y}) - \sigma^2 \tag{10}$$

where $\boldsymbol{\alpha} = \mathrm{diag}\{\boldsymbol{D}\boldsymbol{R}\} = \{[\boldsymbol{D}\boldsymbol{R}]_{1,1}, [\boldsymbol{D}\boldsymbol{R}]_{2,2}, ..., [\boldsymbol{D}\boldsymbol{R}]_{L,L}]\}$ is the vector consisting of diagonal elements of $\boldsymbol{D}\boldsymbol{R}$, $\boldsymbol{g}'(\boldsymbol{D}\boldsymbol{y}) = \boldsymbol{g}'(\boldsymbol{w}) = (\theta_i'(w_i))_{i\in[1;L]}$, $\boldsymbol{D} = [\boldsymbol{D}_1^T, \boldsymbol{D}_2^T, ..., \boldsymbol{D}_J^T]^T$, $\boldsymbol{R} = [\boldsymbol{R}_1, \boldsymbol{R}_2, ..., \boldsymbol{R}_J]$, $\boldsymbol{D}_i$ and $\boldsymbol{R}_i$ are $\boldsymbol{N_i} \times \boldsymbol{N}$ matrix and $\boldsymbol{N} \times \boldsymbol{N_i}$ matrix, $\boldsymbol{\alpha} = [\boldsymbol{\alpha}_1^T, \boldsymbol{\alpha}_2^T, ..., \boldsymbol{\alpha}_J^T]^T$, $\boldsymbol{\alpha}_i = \mathrm{diag}\{\boldsymbol{D}_i\boldsymbol{R}_i\}$. Simply make Eq. (11) in SURE-LET framework which can estimate MSEunbiased.

$$\mathrm{div}\{\boldsymbol{F}(\boldsymbol{y})\} = \boldsymbol{\alpha}^T \boldsymbol{g}'(\boldsymbol{D}\boldsymbol{y}) \tag{11}$$

where $f_n(y) = \sum_{l=1}^{L} r_{n,l}\theta_l(w_l)$, $w_l = \sum_{k=1}^{K} d_{l,k} y_k$. The proof is as shown in Eq. (12):

$$\begin{aligned}
&\mathrm{div}\{\boldsymbol{F}(\boldsymbol{y})\} = \sum_{n=1}^{N} \frac{\partial f_n(\boldsymbol{y})}{\partial y_n} \\
&= \sum_{n=1}^{N}\sum_{l=1}^{L} r_{n,l}\theta_l'(w_l)\frac{\partial w_l}{\partial y_n} \\
&= \sum_{n=1}^{N}\sum_{l=1}^{L} r_{n,l}\theta_l'(w_l) d_{l,n} \\
&= \sum_{l=1}^{L} \theta_l'(w_l)\sum_{n=1}^{N} d_{l,n} r_{n,l}
\end{aligned} \tag{12}$$

$\sum_{n=1}^{N} d_{l,n} r_{n,l} = [\boldsymbol{D}\boldsymbol{R}]_{l,l}$, finally get the conclusion $\mathrm{div}\{\boldsymbol{F}(\boldsymbol{y})\} = \mathrm{diag}\{\boldsymbol{D}\boldsymbol{R}\}^T \boldsymbol{g}'(\boldsymbol{D}\boldsymbol{y})$. That is, the Eq. (11) is established. Among them, the calculation of $\mathrm{diag}\{\boldsymbol{D}\boldsymbol{R}\}$ is the proposed step.

The pointwise threshold function is likely to be efficient if it satisfies the following minimal properties: differentiability, anti-symmetry and linear behavior for large coefficients.

A good choice has been experimentally found to be of the form

$$\begin{aligned}
&g(w) = \theta_i(w) = a_{i,1}t_1(w) + a_{i,2}t_2(w) \\
&t_1(w) = w, t_2(w) = w(1 - e^{-(\frac{w}{3\sigma})^8})
\end{aligned} \tag{13}$$

Similar to what was observed empirically in other settings [41], adding more threshold functions only brings marginal (0.1-0.2 dB) improvement to the overall denoising quality.

Finding the parameters $a_{i,k}$ that minimize the MSE to solve the Eq. (6) and Eq. (7), it is necessary to replace $\boldsymbol{F}(\boldsymbol{y})$ by Eq. (14):

$$\boldsymbol{F}(\boldsymbol{y}) = \sum_i \sum_k a_{i,k}\boldsymbol{F}_{i,k}(\boldsymbol{y}) + \mathrm{lowpass} \tag{14}$$

It should be noted that the I + 1 lowpass band is not processed.

Next, we will summarize the method. And the steps of the Surelet method for seismic signal denoising are as shown in Tab. 1.

Table 1 Detailed steps for seismic signal denoising using the Surelet transform

The processes of denoising seismic signal based on Surelet transform	
(1)	Perform a boundary extension on the noisy seismic signal.
(2)	Perform an undecimated wavelet transform (UWT) on the extended noisy seismic signal.
(3)	Apply the pointwise threshold functions t_k defined in Eq. (13) to the current sub band $\boldsymbol{Wi}$; Reconstruct the processed sub band by setting all the other sub bands to zero to obtain $\boldsymbol{F_{i,k}(y)}$; Compute the first derivative of t_k for each coefficient of the current sub band $\boldsymbol{w}$ and build the corresponding coordinate of $\boldsymbol{c}$ as exemplified by Eq. (6) and Eq. (7).
(4)	Compute the matrix $\boldsymbol{M}$ and deduce the optimal in the minimum SURE sense linear parameters $a_{i,k}$'s using the equations of Eq. (6) and Eq. (7).
(5)	The noise-free seismic signal $\hat{\boldsymbol{X}}$ is finally estimated by the sum of each $\boldsymbol{F_{i,k}}$ weighted by its corresponding SURE-optimized $a_{i,k}$.

The MSE unbiased estimated by SURE-LET can achieve theoretical optimization. This method has an advantage in multi-scale geometric analysis denoising tools. The denoising experiments of the seismic signal are performed below to verify the performance of the SURE-LET.

3.3 Seismic Signal Denoising Experiments

The denoising experiments are performed on a Lenovo ThinkPad laptop with an i5-3320M processor, a CPU of 2.60 GHz, a memory of 4 GB, and a 64-bit Windows operating system. The software platform is MATLAB-R2014b. This study selects a set of parameters for the

algorithms to make the denoising performance the best for each algorithm. The performance of the four algorithms, that is Surelet, Wave Atom, Curvelet and Wavelet is compared based on the metrics such as peak signal-to-noise ratio (PSNR), mean square error (MSE), and denoising time.

$$P_{SNR} = 10\log_{10}\left(\frac{\max(\boldsymbol{y}^2)}{M_{SE}}\right) \tag{15}$$

$$M_{SE} = \frac{1}{mn}\sum_{i=1}^{m}\sum_{j=1}^{n}((\boldsymbol{y}_d - \boldsymbol{y})_{i,j})^2 \tag{16}$$

4 RESULTS AND DISCUSSION

4.1 Synthetic Seismic Signal Denoising

The synthetic seismic signal has a total of 128 traces, each trace contains 128 uniform sampling points. Gaussian white noise with a variance of 20%, 30%, 40%, and 50% is added to the clean signal. Fig. 2 showed the 20% noisy seismic signal and denoising results. The original seismic signal is shown in Fig. 2a, and 2b is the corresponding noisy signal. Now, denoising is performed by using four denoising algorithms.

The Surelet denoising result appears in Fig. 2c. The Wave Atom denoising result is Fig. 2d, and Fig. 2e is the Curvelet denoising. Fig. 2f illustrates the Wavelet denoising result.

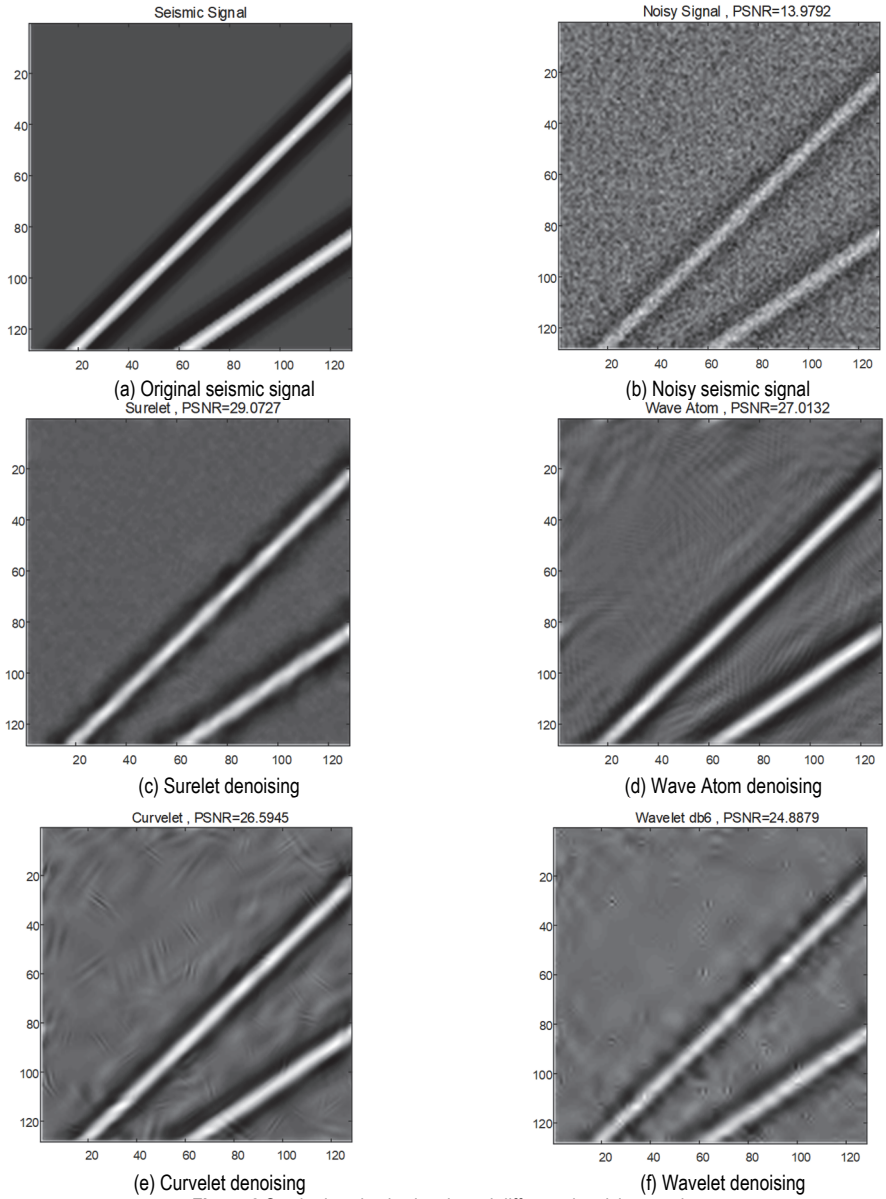

Figure 2 Synthetic seismic signals and different denoising results

Fig. 2 shows the four denoising algorithms basically accomplish the denoising task. Then objectively compare the denoising performance of the four algorithms and find that the PSNR of Surelet and Wave Atom is higher than that of Curvelet and Wavelet. The specific differences in the four denoising performances have been quantified. Tab. 2 listed the denoising performance and runtime of the synthetic seismic signal.

Tab. 2 presents the noise is 20%, Surelet's PSNR is 29.0475, which is 1.7751 more than Wave Atom, which is 6.11% higher, and the running time is 0.201728, which is 78.4% less than the Wave Atom time, which means the

Surelet denoising time is less than half the size of Wave Atom, significantly improving the speed of denoising. With the noise level increaseing, the Surelet denoising effect is optimal. The results show that the Surelet denoising effect is better than Wave Atom, Curvelet and Wavelet, and it also has an advantage in denoising time.

Table 2 Denoising performance and running time of synthetic seismic signals

Noise level	Algorithms	PSNR / dB	MSE	TIME
Sigma = 20%	Surelet	29.0475	0.001245	0.201728
	Wave Atom	27.2724	0.001874	0.933781
	Curvelet	26.4784	0.002250	0.281025
	Wavelet	24.7754	0.003330	0.231749
Sigma = 30%	Surelet	27.1050	0.001948	0.206586
	Wave Atom	25.1492	0.003055	0.938999
	Curvelet	24.2960	0.003719	0.260300
	Wavelet	22.0764	0.006200	0.235495
Sigma = 40%	Surelet	24.7289	0.003366	0.219809
	Wave Atom	23.6708	0.004295	0.954272
	Curvelet	21.9707	0.006352	0.271981
	Wavelet	20.2065	0.009536	0.254763
Sigma = 50%	Surelet	23.2149	0.004770	0.224724
	Wave Atom	22.2524	0.005953	0.965217
	Curvelet	20.4729	0.008968	0.274673
	Wavelet	18.7964	0.013194	0.245212

The proposed method analyzes the Surelet denoising performance better due to the variety of noise, denoising is added to the synthetic seismic signal by adding exponential noise (e = 18, 17, 16, 15). Fig. 3 shows the denoising results for e = 18. The original seismic signal that appears in Fig. 3a, and Fig. 3b is noisy signal. Now denoising is performed using four denoising algorithms.

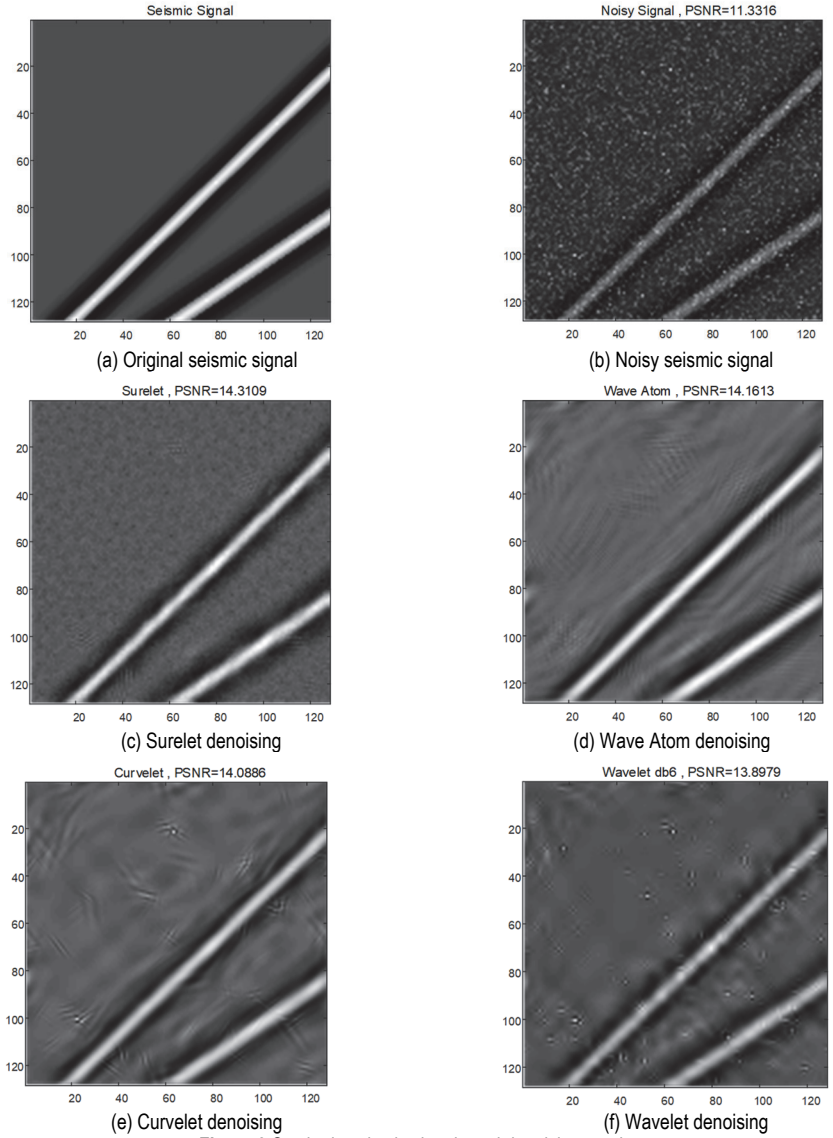

(a) Original seismic signal (b) Noisy seismic signal

(c) Surelet denoising (d) Wave Atom denoising

(e) Curvelet denoising (f) Wavelet denoising

Figure 3 Synthetic seismic signals and denoising results

Fig. 3 indicates the four denoising algorithms can basically complete the denoising task. Tab. 3 lists the metrics of denoising synthetic seismic signal. It is found that the MSE of Surelet and Wave Atom is lower than the Curvelet and Wavelet. The specific differences in the four denoising effects have been quantified.

Table 3 Denoising performance and running time of synthetic seismic signals

Noise level	Algorithms	PSNR / dB	MSE	TIME
$e = 18$	Surelet	14.3109	0.037061	0.213223
	Wave Atom	14.1613	0.038359	0.857448
	Curvelet	14.0886	0.039006	0.240987
	Wavelet	13.8979	0.040758	0.210362
$e = 17$	Surelet	13.8484	0.041225	0.204469
	Wave Atom	13.6105	0.043546	0.889166
	Curvelet	13.4952	0.044718	0.259562
	Wavelet	13.3727	0.045997	0.222004
$e = 16$	Surelet	13.1314	0.048625	0.207911
	Wave Atom	13.0378	0.049685	0.831161
	Curvelet	12.8263	0.052164	0.264723
	Wavelet	12.7451	0.053148	0.215088
$e = 15$	Surelet	12.5159	0.056028	0.203066
	Wave Atom	12.4994	0.056242	0.866926
	Curvelet	12.3190	0.058627	0.272107
	Wavelet	12.2490	0.059580	0.221174

Tab. 3 presents that the metrics of the four algorithms are not much different. When $e = 15$, the PSNR of Surelet is only 0.0165 larger than Wave Atom, and MSE is only 0.003552 less than the Wavelet transform. Surelet has little advantage in removing exponential noise.

This study continues to add uniform noise to the synthetic seismic signal ($a = 0$, $b = 20\%$, 30%, 40%, 50%). Fig. 4 shows the denoising results for $a = 0$ and $b = 20\%$. The original seismic signal is shown in Fig. 4a, and Fig. 4b is noisy signal. Now, denoising is performed using four denoising algorithms. The Surelet denoising result appears in Fig. 4c. The Wave Atom denoising result that appears in Fig. 4d, and Fig. 4e is the Curvelet denoising. Fig. 4f shows the Wavelet denoising result.

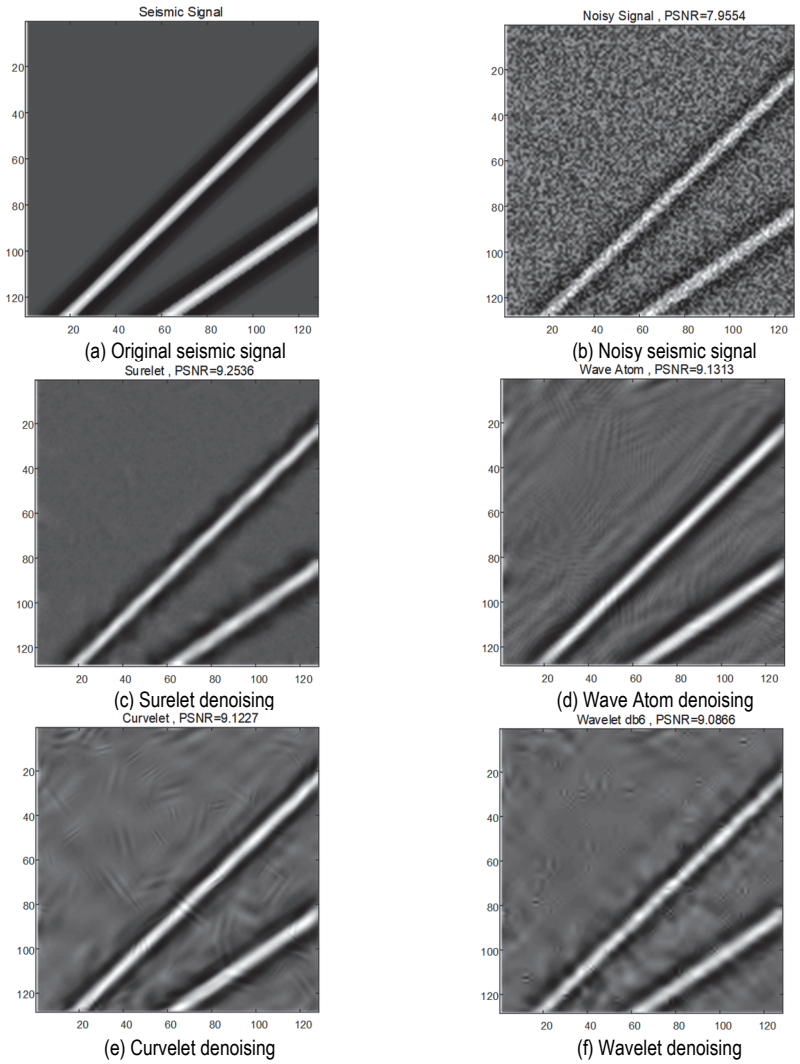

(a) Original seismic signal (b) Noisy seismic signal
(c) Surelet denoising (d) Wave Atom denoising
(e) Curvelet denoising (f) Wavelet denoising

Figure 4 Synthetic seismic signals and denoising results

Fig. 4 shows the four denoising algorithms can basically complete the denoising task. The specific differences in the four denoising performances have been quantified. Tab. 4 lists the metrics of denoising the synthetic seismic signal.

Table 4 Denoising performance and running time of synthetic seismic signals

Noise level	Algorithms	PSNR / dB	MSE	TIME
b = 20%	Surelet	9.2536	0.118752	0.214498
	Wave Atom	9.1313	0.122144	0.948888
	Curvelet	9.1227	0.122385	0.267504
	Wavelet	9.0866	0.123406	0.231551
b = 30%	Surelet	5.6262	0.273765	0.219327
	Wave Atom	5.5738	0.277088	0.975366
	Curvelet	5.5474	0.278781	0.269377
	Wavelet	5.5282	0.280012	0.237361
b = 40%	Surelet	3.1250	0.486970	0.220321
	Wave Atom	3.1014	0.489616	1.033006
	Curvelet	3.0809	0.491935	0.299752
	Wavelet	3.0581	0.494523	0.252069
b = 50%	Surelet	1.2921	0.742663	0.217490
	Wave Atom	1.2845	0.743953	0.959819
	Curvelet	1.2588	0.748383	0.259760
	Wavelet	1.2465	0.750491	0.236057

Tab. 4 shows that the denoising performance of the four algorithms on uniform noise is not obvious, and the difference between the four algorithms is not large.This analysis results show that multi-scale geometric analysis has more obvious advantages in removing Gaussian noise by denoising the signals containing Gaussian noise, exponential noise and uniform noise.This study considers Gaussian noise in the next experiment.

4.2 Marine Seismic Signal Denoising

The marine seismic signal has 256 traces. Each trace contains 256 sampling points. The seismic signal contains the curved events. The events of the complex pre-stack seismic signal are more curved and contain more data, so the denoising is more difficult than experiment 4.1. The original seismic signal which appeared in Fig. 5a, and Fig. 5b is noisy seismic signal with the variance of 20%. Now we remove the noise with Surelet, Wave Atom, Curvelet, and Wavelet.

The Surelet denoising result appeared in Fig. 5c. The Wave Atom denoising result appeared in Fig. 5d, and Fig. 5e is the Curvelet denoising. Fig. 5f showed the Wavelet denoising result and the four denoising algorithms can basically complete the denoising task. But the Surelet denoising results appear to be "clean." The specific differences in the four denoising performances have been quantified. Figs. 6 and 7 are histograms of the PSNR and MSE of the marine seismic signal varying with the noise level.

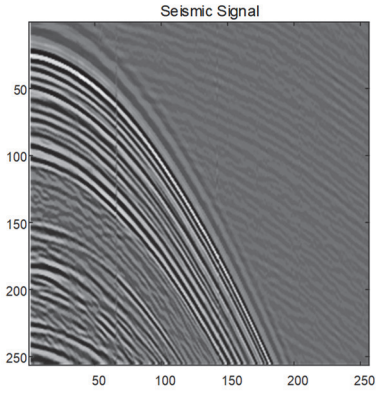

(a) Original seismic signal

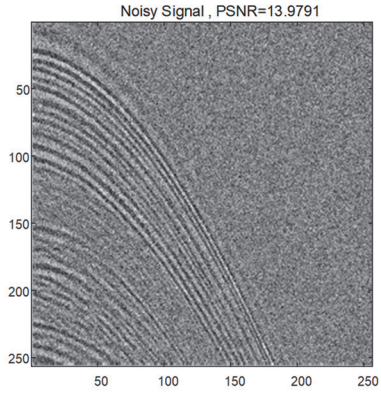

(b) Noisy seismic signal

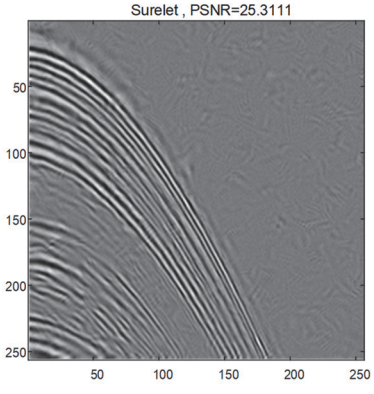

(c) Surelet denoising

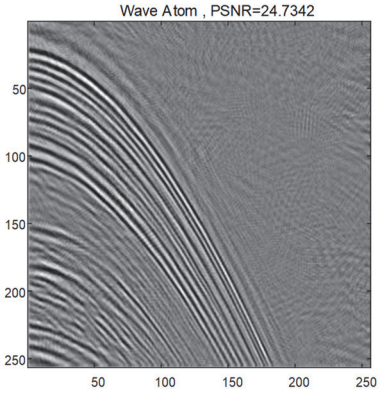

(d) Wave Atom denoising

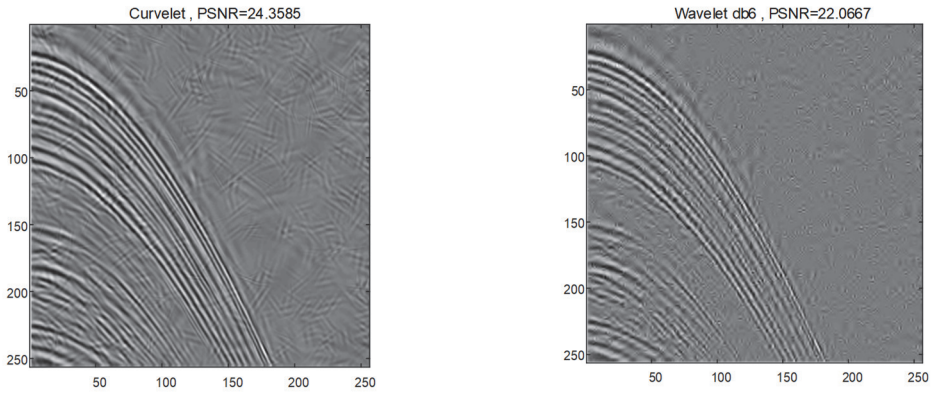

(e) Curvelet denoising (f) Wavelet denoising

Figure 5 Marine seismic signals and denoising results

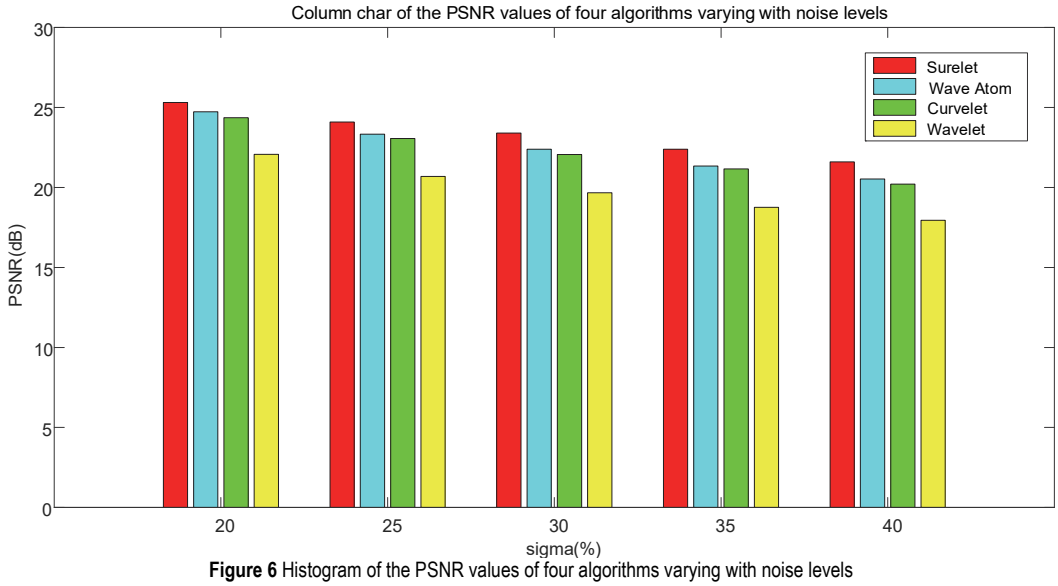

Figure 6 Histogram of the PSNR values of four algorithms varying with noise levels

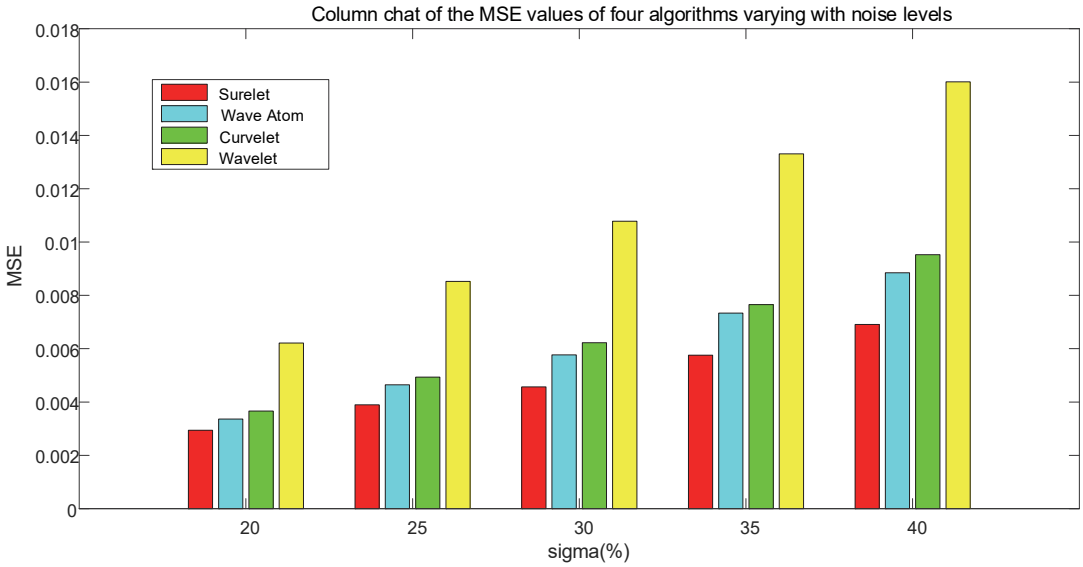

Figure 7 Histogram of the MSE values of four algorithms varying with noise levels

Fig. 6 indicates the Surelet's PSNR is always at its maximum with the noise level changes. Wave Atom and Curvelet are second, and Wavelet is the smallest. Fig. 7 shows Surelet's MSE is always at a minimum with the noise level changes. Then Wave Atom and Curvelet are second, and Wavelet is the largest. Because the Surelet algorithm finds the combination coefficient under the premise that the MSE reaches the approximate minimum through the unbiased risk estimation, and then uses the linear expansion of the threshold to solve the equations, then removes the seismic signal noise. So, the principle of remove noise is simple, and it is easier to denoise the seismic signal.

4.3 3D Seismic Signal Denoising

These experiments present that Surelet has good denoising performance on 2D seismic signals. Now the 3D seismic signal is selected for denoising. The seismic signal has a total of 200 × 200 = 40000 traces, and the single trace contains 200 sampling points.

The three-dimensional seismic signal is cut into 128 × 128 horizontal and vertical slices, and 20%, 25%, 30%, 35% and 40% Gaussian white noise is added to the horizontal and vertical slices of the seismic signal. The denoising process with 20% noise is shown.

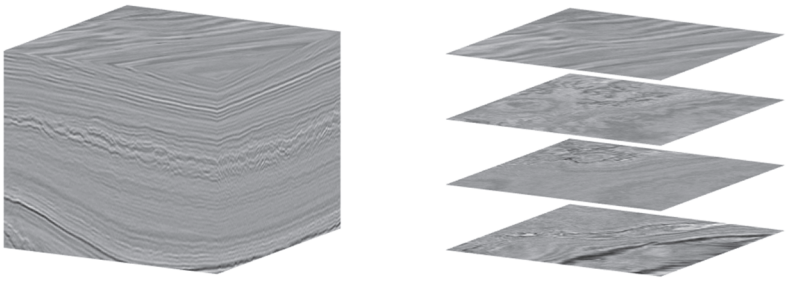

(a) 3D Stereogram (b) 3D Sectional view

Figure 8 Three-dimensional seismic signal

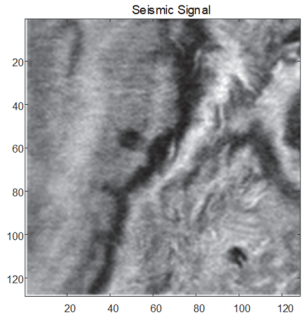

(a) Original three-dimensional horizontal slice

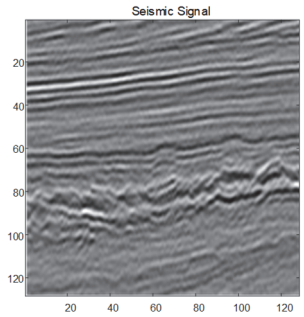

(b) Original three-dimensional vertical slice

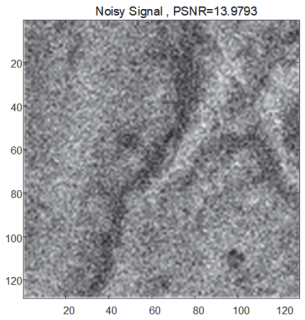

(c) Noisy three-dimensional horizontal slice

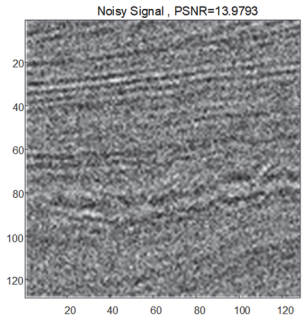

(d) Noisy three-dimensional vertical slice

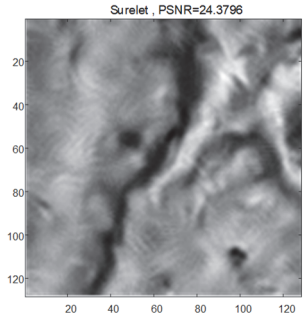

(e) Surelet denoising horizontal slice

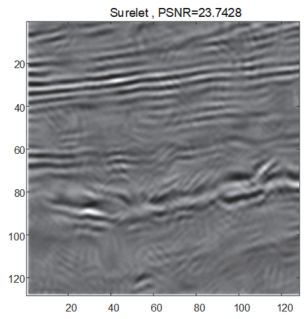

(f) Surelet denoising vertical slice

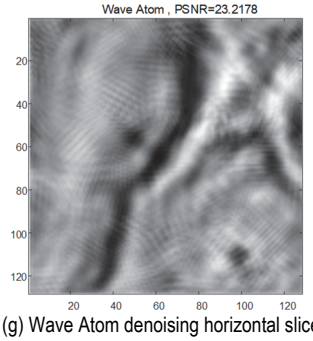

(g) Wave Atom denoising horizontal slice

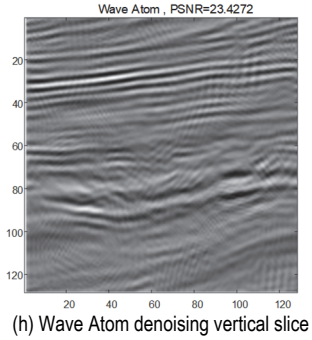

(h) Wave Atom denoising vertical slice

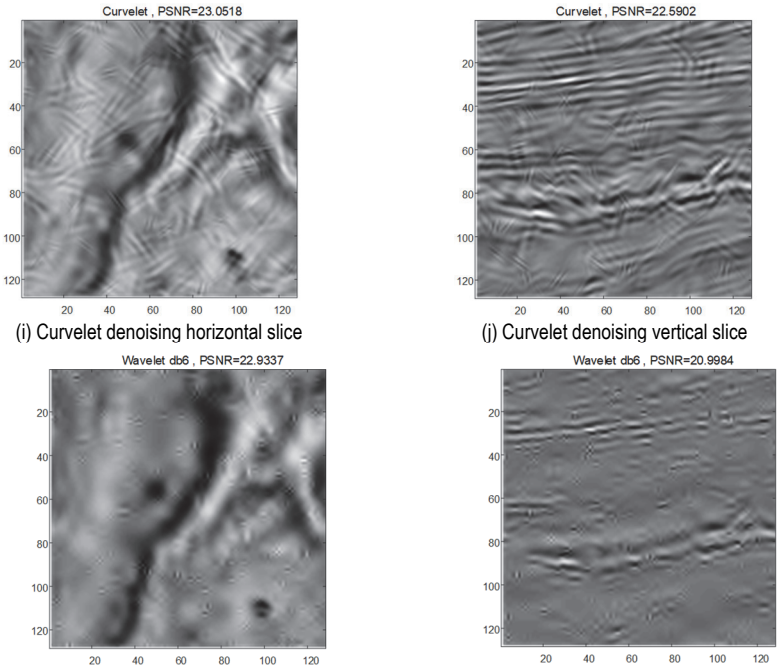

(i) Curvelet denoising horizontal slice (j) Curvelet denoising vertical slice

(k) Wavelet denoising horizontal slice (l) Wavelet denoising vertical slice

Figure 9 Three-dimensional seismic signals and denoising results

The original three-dimensional horizontal slice is shown in Fig. 9a and the original three-dimensional vertical slice is shown in Fig. 9b. The noisy three-dimensional horizontal slice is shown in Fig. 9c and the noisy three-dimensional vertical slice is shown in Fig. 9d. The horizontal slice of the Surelet denoising result appearing in Fig. 9e and Fig. 9f is the vertical slice of Surelet denoising result. The horizontal slice of the Wave Atom denoising result which appears in Fig. 9g, and Fig. 9h is vertical slice of the Wave Atom denoising result. The horizontal slice of the Curvelet denoising result that appeared in Fig. 9i, and Fig. 9j is vertical slice of the Curvelet denoising result. The horizontal slice of the Wavelet denoising result that appeared in Fig. 9k, and Fig. 9l is vertical slice of the Wavelet denoising. As seen in Fig. 9, all four algorithms can attenuate the noise in seismic signal, and specific difference in the denoising performance has been quantified. Figs. 10 and 11 showed the PSNR and MSE of the 3D seismic signal.

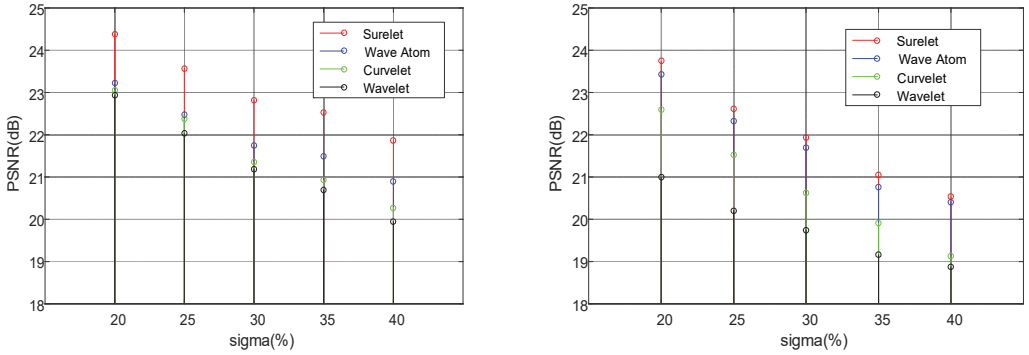

(a) Horizontal slice PSNR of four algorithms (b) Vertical slice PSNR of four algorithms

Figure 10 PSNR of three-dimensional seismic signals

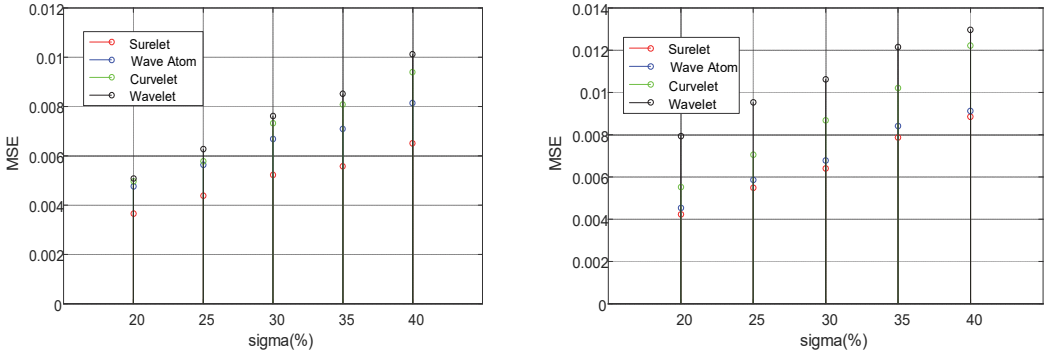

(a) Horizontal slice MSE of four algorithms (b) Vertical slice MSE of four algorithms

Figure 11 MSE of three-dimensional seismic signals

Figs. 10 and 11 show the horizontal slice increases with noise level, and the Surelet's PSNR remains the largest and is noticeably superior compared to the other three approaches. When the noise is 20%, Surelet's PSNR is 24.3796 dB and Wave Atom's PSNR is 23.2178 dB, and performance is increased by 5.0%. Vertical slices increase with noise level, Surelet's PSNR remains the largest, and Wavelet's PSNR is minimal. When the noise is 20%, Surelet's PSNR is 23.7428 dB, Wave Atom's PSNR is 23.4272 dB, Wavelet's PSNR is 20.9984 dB, Surelet performance is 1.3% higher than Wave Atom, and 13.1% higher than Wavelet. The analysis shows that Surelet's denoising performance on 3D seismic signals is better than Wave Atom, Curvelet and Wavelet. Surelet is also the fastest in denoising time, which effectively shortens the denoising time and reduces the MSE. Therefore, it has an advantage in the denoising of 3D seismic signals.

4.4 Discussion

Seismic signal denoising is to lower the resource usage and lower the environmental impacts. It is an important step in energy exploration. But no one has used Surelet transform for seismic signal denoising till now. Stein's unbiased risk estimation linear extended threshold algorithm (Surelet) uses mathematical transform to solve the combined coefficients of MSE approximation minimum, then complete the seismic signal denoising. The Surelet transform is used to denoise two-dimensional and three-dimensional seismic signals in the experiments. The outcomes reveal that denoising performance is improved compared with some classical multi-scale geometric analysis denoising algorithms. There are several key contributions addressed from this research:

(1) Applying Surelet in multi-scale geometric analysis to energy exploration and achieving good performance in the results;

(2) Denoising the two-dimensional seismic signals with Surelet, Wave Atom, Curvelet and Wavelet. The PSNR and the running time, Surelet has the best denoising performance and fast denoising speed. It is precisely because SURE has the characteristic of optimal threshold selection that the improved PSNR aligns with [40]. Wave Atom's denoising performance is between Surelet and Curvelet; still, the Wavelet's denoising performance is poor. Surelet has the advantage of denoising two-dimensional seismic signals;

(3) Denoising the three-dimensional seismic signals with Surelet, Wave Atom, Curvelet and Wavelet. In terms of denoising performance, Surelet is the best and Wave Atom is second. Wavelet has the lowest denoising performance. For denoising speed, Surelet transform is the fastest, wavelet transform is the second, and the wave atom transform is the slowest. Surelet improves denoising performance without compromising long periods of time.

This study is necessary to find a fast and simple algorithm to enhance the performance of seismic signal denoising, which plays crucial role in subsequent seismic data analysis and energy exploration.

This study also encountered limitations, which can denoise seismic signals with the same trace number and sampling point. For example, the seismic signal with trace number of 2nd power can be denoised, however the irregular seismic signal fails to remove. Another limitation is that it poses certain challenge in processing complex 3D data. Alternate methods like Surelet may potentially improve parameter selection problem.

The future study might optimize the algorithm to enhance the performance of seismic signal denoising based on Surelet transform for energy exploration.

5 CONCLUSION

This study proposed using the Surelet transform for efficient seismic denoising in energy exploration. Experiments on synthetic 2D and 3D seismic signals demonstrated improved peak signal-to-noise ratios and faster processing compared to wavelet, curvelet, and wave atom techniques. The optimal thresholds identified by SURE combined with linear expansion estimation enabled effective noise removal while retaining signal features. Limitations of the approach include sensitivity to parameter selection and computational complexity for 3D data. Overall, the feasibility of Surelet seismic denoising was shown, highlighting its potential to extract cleaner signals for improved subsurface characterization. Future work should focus on parameter optimization and efficient implementations.

6 REFERENCES

[1] Wu, Y., Gao, G., & Cui, C. (2019). Improved wavelet denoising by non-convex sparse regularization under double wavelet domains. *IEEE Access*, *7*, 30659-30671. https://doi.org/10.1109/ACCESS.2019.2903125

[2] Li, J., Zhang, Y., Qi, R., & Liu, Q. (2017). Wavelet-based higher order correlative stacking for seismic data denoising in the curvelet domain. *IEEE Journal of Selected Topics in Applied Earth Observations and Remote Sensing*, *10*(8), 3810-3820. https://doi.org/10.1109/JSTARS.2017.2685628

[3] Wang, X. & Ma, J. (2020). Adaptive dictionary learning for blind seismic data denoising. *IEEE Geoscience and Remote Sensing Letters*, *17*(7), 1273-1277. https://doi.org/10.1109/LGRS.2019.2941025

[4] Yuan, S., Wang, S., Luo, C., & Wang, T. (2018). Inversion-Based 3-D seismic denoising for exploring spatial edges and spatio-temporal signal redundancy. *IEEE Geoscience and Remote Sensing Letters*, *15*(11), 1682-1686. https://doi.org/10.1109/LGRS.2018.2854929

[5] Yamate, T., Fujisawa, G., & Ikegami, T. (2017). Optical sensors for the exploration of oil and gas. *Journal of Lightwave Technology*, *35*(16), 3538-3545. https://doi.org/10.1109/JLT.2016.2614544

[6] Huang, W., Wu, R., & Wang, R. (2018). Damped Dreamlet representation for exploration seismic data interpolation and denoising. *IEEE Transactions on Geoscience and Remote Sensing*, *56*(6), 3159-3172. https://doi.org/10.1109/TGRS.2018.2793856

[7] Prashar, A. (2019). Towards sustainable development in industrial small and Medium-sized Enterprises: An energy sustainability approach. *Journal of Cleaner Production*, *235*, 977-996. https://doi.org/10.1016/j.jclepro.2019.07.045

[8] Bai, M., Chen, W., & Chen, Y. (2019). Nonstationary least-squares decomposition with structural constraint for denoising multi-channel seismic data. *IEEE Transactions on Geoscience and Remote Sensing*, *57*(12), 10437-10446. https://doi.org/10.1109/TGRS.2019.2935799

[9] Liu, N., Li, W., Tao, R., & Fowler, J. (2019). Wavelet-domain low-rank/group-sparse destriping for hyperspectral imagery. *IEEE Transactions on Geoscience and Remote Sensing*, *57*(12), 10310-10321. https://doi.org/10.1109/TGRS.2019.2933555

[10] Kamble, V., Parlewar, P., Keskar, A., & Bhurchandi, K. (2016). Performance evaluation of wavelet, ridgelet, curvelet

and contourlet transforms based techniques for digital image denoising. *Artificial Intelligence Review*, *45*(4), 509-533. https://doi.org/10.1007/s10462-015-9453-7

[11] Latif, A. & Mousa, W. (2017). An efficient under sampled high-resolution radon transform for exploration seismic data processing. *IEEE Transactions on Geoscience and Remote Sensing*, *55*(2), 1010-1024. https://doi.org/10.1109/TGRS.2016.2618848

[12] Le, E. & Mallat, S. (2002). Image compression with geometrical wavelets. *Proceedings 2000 International Conference on Image Processing, Vancouver, BC, Canada*. https://doi.org/10.1109/ICIP.2000.901045

[13] Candès, E., &Donoho, D. (2004). New tight frames of curvelets and optimal representations of objects with piecewise c^2 singularities. *Communications on pure and applied mathematics*, *57*(2), 219-266. https://doi.org/10.1002/cpa.10116

[14] Do, M. & Vetterli, M. (2005). The contourlet transform: An efficient directional multiresolution image representation. *IEEE Transactions on Image Processing*, *14*(12), 2091-2106. https://doi.org/10.1109/TIP.2005.859376

[15] Guo, K. & Labate, D. (2007). Optimally sparse multidimensional representation using shearlets. *Siam Journal Mathematical Analysis*, *39*(1), 298-318. https://doi.org/10.1137/060649781

[16] Tseng, M., Islam, M., Karia, N., Fauzi, F., & Afrin, S. (2019). A literature review on green supply chain management: Trends and future challenges. *Resources Conservation and Recycling*, *141*, 145-162. https://doi.org/10.1016/j.resconrec.2018.10.009

[17] Tseng, M., Chiu, A., & Ashton, W. (2019). Sustainable management of natural resources toward sustainable development goals. *Resources Conservation and Recycling*, *145*, 419-421. https://doi.org/10.1016/j.resconrec.2019.03.012

[18] Rong, Q. & Qiao, X. (2019). FBG for oil and gas exploration. *Journal of Light wave Technology*, *37*(11), 2502-2515. https://doi.org/10.1109/JLT.2018.2866326

[19] Raj, J., Vijayalakshmi, K., & Priya, S. (2019). Medical image denoising using multi-resolution transforms. *Measurement*, *145*, 769-778. https://doi.org/10.1016/j.measurement.2019.01.001

[20] Meyer, F. & Coifman, R. (1997). Brushlets: A tool for directional image analysis and image compression. *Applied and Computational Harmonic Analysis*, *4*(2), 147-187. https://doi.org/10.1006/acha.1997.0208

[21] Donoho, D. (1999). Wedgelets: Nearly minimax estimation of edges. *The Annals of Statistics*, *27*(3), 859-897. https://doi.org/10.2307/120143

[22] Le, E. & Mallat, S. (2005). Sparse geometric image representations with Bandelets. *IEEE Transactions on Image Processing*, *14*(4), 423-438. https://doi.org/10.1109/TIP.2005.843753

[23] Candès, E. (1998). Ridgelets: Theory and applications. *Stanford University, USA: Depart-ment of Statistics*.

[24] Donoho, D. (2000). Orthonormal ridgelets and linear singularities. *Siam Journal on Mathematical Analysis*, *31*(5), 1062-1099. https://doi.org/10.1137/S0036141098344403

[25] Candès, E. (1999). Monoscale Ridgelets for the Representation of Images with Edges. *Stanford University, USA: Department of Statistics*.

[26] Candès, E. & Donoho, D. (1999). Curvelets. *Stanford University, USA: Department of Statistics*.

[27] Candès, E. & Donoho, D. (1999). Curvelets: A surprisingly effective nonadaptive representation for objects with edges. *Curves and Surface, Nashville: Vanderbilt University Press, USA*, 123-143.

[28] Do, M. & Vetterli, M. (2003). Contourlets. *Studies in Computational Mathematics*, *10*(3), 83-105. https://doi.org/10.1016/S1570-579X(03)80032-0

[29] Zhang, W., Liu, F., Jiao, L., Hou, B., Wang, S., & Shang, R. (2010). SAR Image despeckling using edge detection and feature clustering in Bandelet domain. *IEEE Geoscience and Remote Sensing Letters*, *7*(1), 131-135. https://doi.org/10.1109/LGRS.2009.2028588

[30] Sadreazami, H., Ahmad, M., & Swamy, M. (2016). A study on image denoising in contourlet domain using the alpha-stable family of distributions. *Signal Processing*, *128*, 459-473. https://doi.org/10.1016/j.sigpro.2016.05.018

[31] Zhang, C., Chen, Y., Duanmu, C., & Yang, Y. (2016). Image denoising by using PDE and GCV in tetrolet transform domain. *Engineering Applications of Artificial Intelligence*, *48*, 204-229. https://doi.org/10.1016/j.engappai.2015.10.008

[32] Yang, G., Lu, Z., Yang, J., & Wang, Y. (2019). An Adaptive contourlet HMM-PCNN model of sparse representation for image denoising. *IEEE Access*, *7*, 88243-88253. https://doi.org/10.1109/ACCESS.2019.2924674

[33] Wang, X., Yin, L., Gao, M., Wang, Z., Shen, J., & Zou, G. (2019). Denoising method for passive photon counting images based on Block-Matching 3D filter and non-subsampled contourlet transform. *Sensors*, *19*(11), 2462. https://doi.org/10.3390/s19112462

[34] Tang, G., & Ma, J. (2011). Application of Total-Variation based curvelet shrinkage for three-dimensional seismic data denoising. *IEEE Geoscience and Remote Sensing Letters*, *8*(1), 103-107. https://doi.org/10.1109/LGRS.2010.2052345

[35] Al-Marzouqi, H. & Al-Regib, G. (2017). Curvelet transform with learning-based tiling. *Signal Processing-Image Communication*, *53*, 24-39. https://doi.org/10.1016/j.image.2017.01.009

[36] Bai, M., Wu, J., Zhang, M., & Chen, Y. (2019). Least-squares Gaussian beam transform for seismic noise attenuation. *IEEE Transactions on Geoscience and Remote Sensing*, *57*(11), 8685-8694. https://doi.org/10.1109/TGRS.2019.2922364

[37] Zhang, H., Chen, X., & Zhang, L. (2017). 3D simultaneous seismic data reconstruction and noise suppression based on the curvelet transform. *Applied Geophysics*, *14*(1), 87-95. https://doi.org/10.1007/s11770-017-0607-z

[38] Zhang, C. & Vanderbaan, M. (2018). Multicomponent microseismic data denoising by 3D shearlet transform. *Geophysics*, *83*(3), A45-A51. https://doi.org/10.1190/GEO2017-0788.1

[39] Tang, N., Zhao, X., Li, Y., & Zhu, D. (2018). Adaptive threshold shearlet transform for surface microseismic data denoising. *Journal of Applied Geophysics*, *153*, 64-74. https://doi.org/10.1016/j.jappgeo.2018.03.019

[40] Blu, T. & Luisier, F. (2007). The SURE-LET approach to image denoising. *IEEE Transactions on Image Processing*, *16*(11), 2778-2786. https://doi.org/10.1109/TIP.2007.906002

[41] Luisier, F., Blu, T., & Unser, M. (2007). A New SURE Approach to Image Denoising: Interscale Orthonormal Wavelet Thresholding. *IEEE Transactions on Image Processing*, *16*(3), 593-606. https://doi.org/10.1109/TIP.2007.891064

[42] Liang, M., Du, J., & Liu, H. (2014). Self-adaptive spatial image denoising model based on scale correlation and SURE-LET in the nonsubsampled contourlet transform domain. *Science China-Information Sciences*, 57(9), 092106. https://doi.org/10.1007/s11432-013-4943-1

Contact information:

Mu DING, Doctoral Student
(Corresponding author)
School of Electronics and Information Engineering,
Hebei University of Technology,
5340 Xiping Road, Beichen District, Tianjin 300401, China
E-mail: 594931107@qq.com